

# Sensitivity Analysis of Piezoelectric Microcantilever Excitability as Resonator

**Reza Ghaderi<sup>1</sup>**

Department of Mechanical Engineering, Shahrekord Branch, Islamic Azad University, Sharekord, Iran

E.mail: Reza.Ghaderi@ymail.com

**Received: 28 October 2022, Revised: 24 January 2023, Accepted: 21 February 2023**

**Abstract:** Piezoelectric Microcantilevers (MCs) are efficient tools in switches of MEMS, AFMs and nano-resonators. Creating maximum vibrating motion with minimum excitation voltage is important in reducing power consumption and noise in this type of MCs. Therefore, investigating the factors affecting the excitability of MCs, as well as the degree of the effect of each of these factors, have an important role in the design and optimal selection of this type of resonators. Therefore, the aim of this paper was to investigate the excitability of this type of MCs. Modeling is conducted according to Hamilton principle and Euler-Bernoulli theory. Equation of motion was solved using Galerkin method with respect to geometrical discontinuities. Finally, eFAST sensitivity analysis was performed on excitability of MCs using statistical methods. Sensitivity analysis results show that the length and thickness of the piezoelectric layer are the most influential parameters on the excitability of MCs. At  $L_1/L=0.74$ , the excitability reaches its maximum value.

**Keywords:** Excitation Ability, Piezoelectric Microcantilever, Sensitivity Analysis

**Biographical note:** Reza Ghaderi is Associate Professor of Mechanical Engineering at the Islamic Azad University, Shahrekord Branch, Iran, where he has been involved in teaching and research activities in the area of vibration for the last 15 years. He received his PhD in Mechanical Engineering from Islamic Azad University, Science and Research Branch, Tehran, Iran in 2013. His current research focuses on nonlinear vibration of piezoelectric MCs, atomic force microscope and microelectromechanical systems.

Research paper

COPYRIGHTS

© 2023 by the authors. Licensee Islamic Azad University Isfahan Branch. This article is an open access article distributed under the terms and conditions of the Creative Commons Attribution 4.0 International (CC BY 4.0)

<https://creativecommons.org/licenses/by/4.0/>



1 INTRODUCTION

MCs are extensively used in AFM [1-2], mass sensing [3-5], nano-manipulation [6-7], imaging surfaces with nanometer resolution [8] and MEMS switches [9-10] because they are highly flexible, sensitive to atomic and molecular force, and fast in response. MCs are also used as micro-and nano-resonators in medical diagnostics, environmental safety and national security settings [11-12]. Among MCs, piezoelectric MCs are known as the new generation and can be used in imaging AFM [13], bio mass sensing[14-15]. The advantage of this type of MCs compared to other cantilevers (without piezoelectric layer) is that they can be used as a self-actuator, self-sensor, and self-actuator self-sensor simultaneously. When they are used as the actuator, these MCs provide more bandwidth compared to regular piezotubes [16]. Therefore, they are suitable for higher speed imaging in AFM. If one uses piezoelectric MC as a sensor, an accuracy equal to laser measurement can be obtained [17], therefore the piezoelectric MCs can replace laser system in AFMs. Therefore, disadvantages such as expensive lasers, large space needed for lasers, and problems in liquid environments can be solved.

Modeling the piezoelectric vibrating motion of MC has been considered in previous studies. Wolf and Gottlieb [18] studied vibrating motion of a MC with an overall piezoelectric layer in non-contact mode of AFM using multiple time scale (MTS) method. Fung and Huang [19] used the finite element to model piezoelectric MC in non-contact mode. Mahmoodi and Jalili [20-21] used the non-linear vibration theory to study the vibrating motion of a piezoelectric cantilever. They studied cantilever with piecewise piezoelectric layer containing geometric discontinuities, they used uniform beam method in vibration modeling.

Mahmoodi and Jalili [22] used MTS method to drive 2x and 3x resonance subharmonics of piezoelectric MCs and compared the results with experimental results. The main body of MCs is usually made wider due to the presence of piezoelectric layer. Tip is selected with narrower section to enhance the sensitivity of the bending [21]. Therefore, MC has two discontinuities. The first discontinuity is at the piezoelectric layer and the second discontinuity is where the MC becomes narrower. Salehi-Khojin [23] modeled piezoelectric MC using non-uniform beam method and compared the results with the experimental results. They showed that this model has good accuracy in the simulation MC piezoelectric.

The vibrating motion of the resonator is important, and creating maximum amplitude using minimum excitation is an important factor in the optimum design of this equipment. Therefore, in this paper, sensitivity analysis of the excitability of piezoelectric MC is investigated for

the first time. Sensitivity analysis aimed at understanding the performance of piezoelectric MCs and investigating the effects of geometry on their performance. Sensitivity analysis can help to optimize the geometry of piezoelectric MCs, in which the excitability of MC is maximized. For this purpose, differential Equations governing the motion of the piezoelectric MCs are solved considering the geometric discontinuities, and then, sensitivity analysis is conducted on the excitability of MCs using the eFAST method.

2 DYNAMIC MODELING OF MC

Discontinuous MC that shown in “Fig. 1” is selected for the dynamic modeling. Piezoelectric layer is a mechanical part, which is bent by applying an electrical voltage, thus, it can bend the MC by applying stress. This layer is located on the MC and is surrounded by two electrodes.

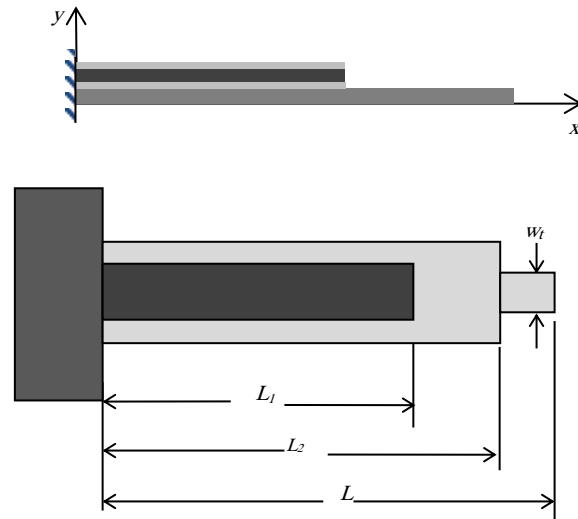


Fig. 1 Schematic view of piezoelectric MC.

Using Hamilton's principle and the Euler-Bernoulli theory, Equation of motion of a piezoelectric MC can be obtained as follows [3]:

$$m(x) \frac{\partial^2 v}{\partial t^2} + \frac{\partial^2}{\partial x^2} \left[ K(x) \frac{\partial^2 v}{\partial x^2} \right] + P(t) \frac{\partial^2 C_e(x)}{\partial x^2} = 0 \quad (1)$$

Where:

$$m = m_1(H_0 - H_{L_1}) + m_2(H_{L_1} - H_{L_2}) + m_3(H_{L_2} - H_L) \quad (2)$$

$$m_1 = \sum_{i=1}^4 \rho_i h_i b_i; m_2 = \rho_1 h_1 b_1; m_3 = \rho_1 h_1 b_t \quad (3)$$

$$K = (EI)_1(H_0 - H_{L_1}) + (EI)_2(H_{L_1} - H_{L_2}) + (EI)_3(H_{L_2} - H_L) \quad (4)$$

$$C_e = E_3 d_{31} b_3 \left( h_1 + h_2 + \frac{1}{2} h_3 - y_n \right) (H_0 - H_{L_1}) \quad (5)$$

$$(EI)_1 = \sum_{k=1}^4 E_k b_k h_k \left\{ \frac{h_k^2}{12} + \left[ y_n - \left( \sum_{j=1}^k h_j - \frac{h_k}{2} \right) \right]^2 \right\}; \quad (6)$$

$$(EI)_2 = E_2 \frac{b_1 h_1^3}{12}; \quad (EI)_3 = E_1 \frac{b_t h_1^3}{12}$$

$$y_n = \frac{\sum_{i=1}^4 E_i w_i h_i \left( \sum_{j=1}^i h_j - \frac{h_i}{2} \right)}{\sum_{i=1}^4 E_i w_i h_i} \quad (7)$$

Where  $H_{L_i}$  is the Heaviside function:

$$H_{L_i} = H(x - L_i) \quad (8)$$

The electrical voltage, which is applied to the piezoelectric layer and bends the MC, enters the Equation of motion of MC through the electromechanical coupling coefficient,  $C_e$ . The governing Equation can be solved using the separation of variables:

$$v(x, t) = \sum_{n=1}^{\infty} \Phi_n(x) q_n(t) \quad (9)$$

Where,  $q_n$  are generalized time-dependent coordinates, and  $\Phi_n$  is the  $n^{\text{th}}$  mode shape. Due to the geometrical discontinuities, the MC has to be divided into three homogeneous beams to improve the accuracy of calculations. The first part of MC includes piezoelectric layer and electrodes, the second part does not include piezoelectric layer, and the third part is the tip. Accordingly,  $\Phi_n$  can be expressed in the following form:

$$\Phi_n(x) = \begin{cases} \varphi_{1n}(x) & 0 \leq x \leq L_1 \\ \varphi_{2n}(x) & L_1 \leq x \leq L_2 \\ \varphi_{3n}(x) & L_2 \leq x \leq L \end{cases} \quad (10)$$

Where:

$$\varphi_{in}(x) = A_{in} \sin \beta_{in} x + B_{in} \cos \beta_{in} x + C_{in} \sin \beta_{in} x + D_{in} \cosh \beta_{in} x \quad (11)$$

$\beta_{in} = (\omega_n^2 m_i / (EI)_i)^{1/4}$ ,  $A_{in}$ ,  $B_{in}$ ,  $C_{in}$  and  $D_{in}$  are constants which can be obtained by the boundary conditions of MC, the continuity conditions, as well as normalization condition with respect to mass in each vibrating mode. Boundary conditions and continuity of beam in each stepped point are:

$$\begin{aligned} \varphi_{1n}(0) &= 0; \varphi_{1n}'(0) = 0; \\ \varphi_{3n}(L) &= 0; \varphi_{3n}''(L) = 0 \\ \varphi_{1n}(L_1) &= \varphi_{2n}(L_1); \varphi_{1n}'(L_1) = \varphi_{2n}'(L_1); \\ \varphi_{2n}(L_2) &= \varphi_{3n}(L_2); \varphi_{2n}''(L_2) = \varphi_{3n}''(L_2); \\ (EI)_1 \varphi_{1n}''(L_1) &= (EI)_2 \varphi_{2n}''(L_1); \\ (EI)_1 \varphi_{1n}'''(L_1) &= (EI)_2 \varphi_{2n}'''(L_1); \\ (EI)_2 \varphi_{2n}''(L_2) &= (EI)_3 \varphi_{3n}''(L_2); \\ (EI)_2 \varphi_{2n}'''(L_2) &= (EI)_3 \varphi_{3n}'''(L_2). \end{aligned} \quad (12)$$

Substituting ‘‘Eq. (12)’’ into ‘‘Eq. (11)’’ results in the formation of the characteristics matrix Equation which can be expressed as:

$$Jacob_{12 \times 12} \times H_{12 \times 1} = 0 \quad (13)$$

Where  $H$  is vector of mode shape coefficients:

$$H = [A_{1n} B_{1n} C_{1n} D_{1n} A_{2n} B_{2n} C_{2n} D_{2n} A_{3n} B_{3n} C_{3n} D_{3n}] \quad (14)$$

And  $Jacob$  is the characteristics matrix given in appendix. Solving  $\det[Jacob]=0$  leads to the derivation of natural frequencies. Separating the variables of the differential Equation of motion using ‘‘Eq. (9)’’ gives:

$$\ddot{q}_n + \omega_n^2 q_n + \mu_n \dot{q}_n + J \cdot P(t) = 0 \quad (15)$$

where:

$$\omega_n^2 = \int_0^1 \varphi_n(K(x) \varphi_n'')' dx \quad (16)$$

$$\mu_n = 2\xi_n \omega_n \quad (17)$$

$$J = \int_0^1 \varphi_n C_e''(x) dx \quad (18)$$

The ordinary differential Equation of motion (15) for  $k$  modes can be written in matrix form as:

$$M\ddot{q} + C\dot{q} + Kq = F \quad (19)$$

Where:

$$\begin{aligned} q &= [q_1(t), q_2(t), \dots, q_k(t)]_{k \times 1}^T; \quad M = I_{k \times k}; \quad C = [C_{km}]_{k \times k}; \\ K &= [\omega_k^2 \delta_{km}]_{k \times k}; \quad F = [-P(t)J_1, \dots, -P(t)J_k]_{k \times 1}^T \end{aligned} \quad (20)$$

The steady state representation of “Eq. (19)” can be written as:

$$\dot{Y} = AY + B \tag{21}$$

In which:

$$A = \begin{bmatrix} 0 & I \\ M^{-1}K & M^{-1}C \end{bmatrix}_{2k \times 2k}; B = \begin{bmatrix} 0 \\ M^{-1}F \end{bmatrix}_{2k \times 1}; Y = \begin{bmatrix} q \\ \dot{q} \end{bmatrix}_{2k \times 1} \tag{22}$$

By using numerical methods, “Eq. (21)” can be solved. Here, the Runge-Kutta method is used in Matlab.

### 3 SENSITIVITY ANALYSIS OF EXCITABILITY

An important factor in piezoelectric MCs is their excitability. Certainly the higher the excitability of MCs, the less input energy is needed to create a higher amplitude. This not only reduces power consumption of MCs, but also reduces the input noise. Since piezoelectric beams are self-actuator, their excitability depends on beam geometry and material. To achieve the higher excitability, MC geometry has to be chosen optimally.

Sensitivity analysis is a method for optimization that can be used in all sciences and optimization projects. It can be used to analyze the effect of inputs on output. In this section, sensitivity analysis is aimed at understanding how a piezoelectric MC functions and at calculating optimum geometrical dimensions to achieve maximum excitability in this type of resonators. Since the excitability of these MCs depends on the geometric parameters, statistical methods have to be utilized to perform sensitivity analysis. One of the best and most accurate methods is eFAST method, which is used in this study. In “Eq. (14)”, the coefficient  $J$  is excitation coefficient. Sensitivity analysis is performed on this coefficient to evaluate the excitability.

Figure 2 shows the effects of MC base layer geometry on excitability. Since excitability depends on  $C_e$ , and this coefficient is directly correlated with the thickness of the MC base layer, it is expected that increasing the thickness of this layer increases excitability. “Fig. 2a” shows that excitability increases with increase in thickness. However, increase in thickness of the base layer increases the rigidity of MC, and as a result, reduces its amplitude. Therefore, despite the fact that this geometric characteristic increases the excitability, it cannot be considered as an appropriate parameter in optimizing piezoelectric MC. As can be seen in “Fig. 2b”, the width of this layer has no significant effect on excitability, and increasing it slightly reduces

excitability. According to the results (“Fig. 2c”), the best length for the base layer is about 490 micrometers, in which the excitability reaches its peak.

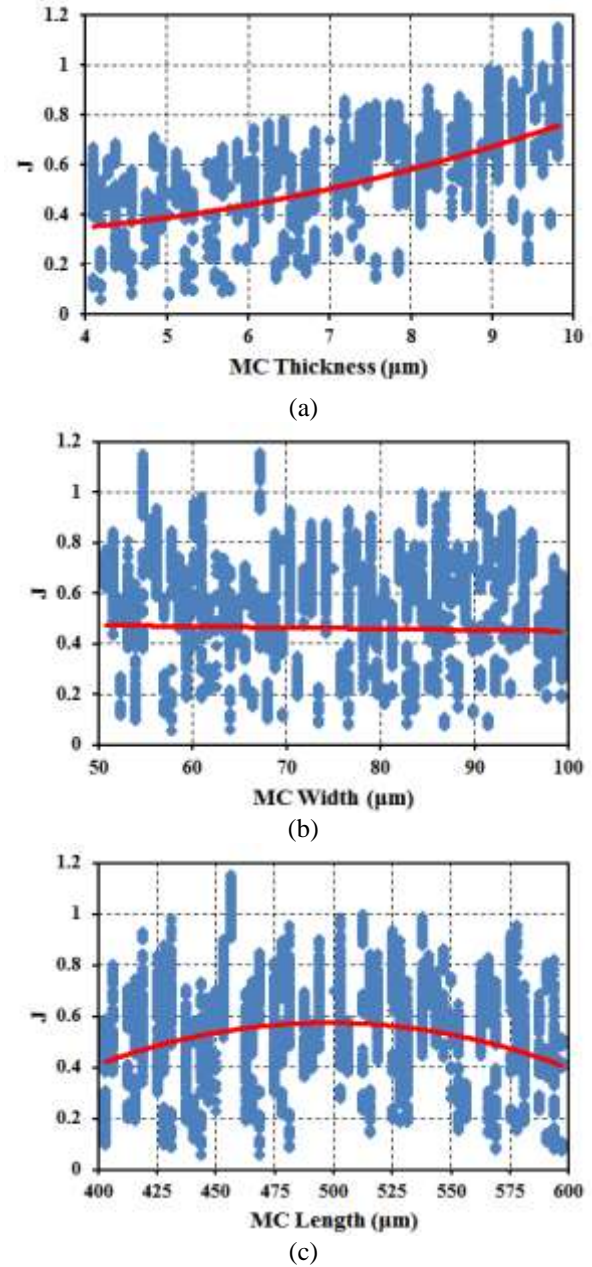


Fig. 2 Effect of the geometric dimensions of the base layer on the excitability of the MC.

Effect of the geometric dimensions of the piezoelectric layer on excitability of MC is shown in Figure 3. As can be seen, the increase in thickness and width of the piezoelectric layer increases the excitability as well. Comparing the results of “Figs. 3a and 2a” shows that the effect of base layer thickness is more significant than thickness of the piezoelectric layer. Although the

increase in piezoelectric layer thickness increases the excitability of MC, resonance amplitude of MC decreases by increasing its rigidity. According to “Fig. 3c”, increasing the length of piezoelectric layer increases excitability. Excitability reaches its maximum value at  $L_1/L=0.74$ .

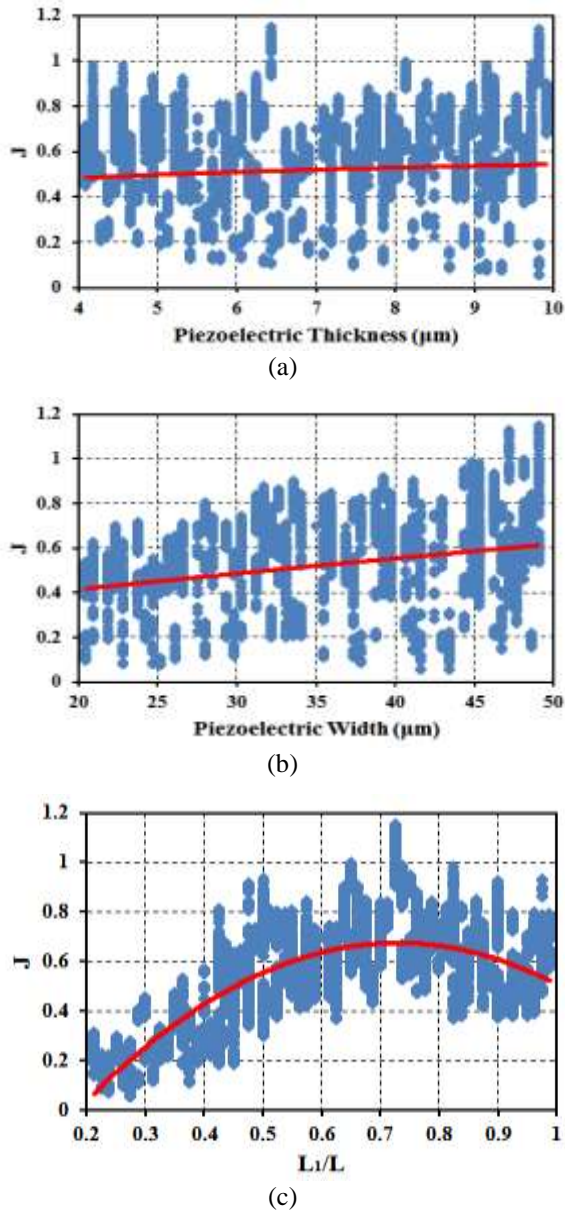


Fig. 3 Effect of the geometric dimensions of the piezoelectric layer on excitability.

Figure 4 shows the effects of width and length of the tip on excitability. According to the results, to enhance the excitability, it is recommended to select a narrow and long tip for MC.

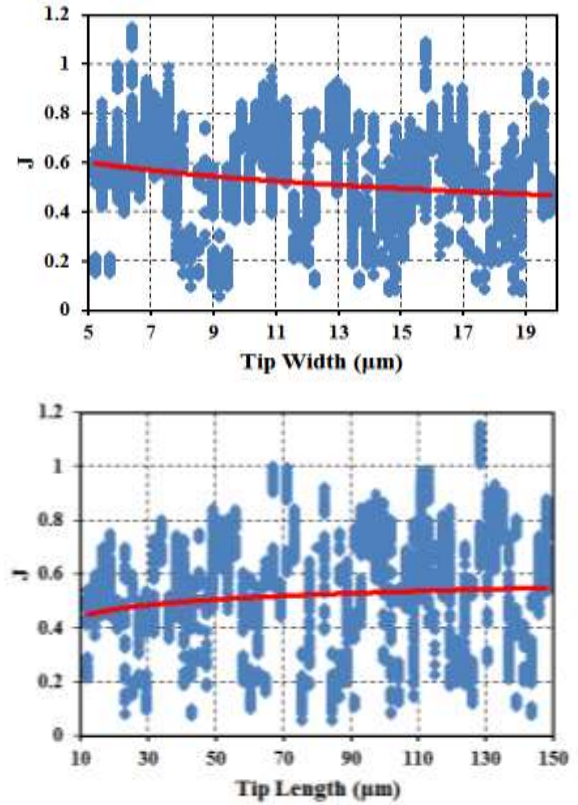


Fig. 4 Effect of width and length of the tip on excitability.

Sensitivity percentage of MC excitability to each of the geometric dimensions is shown in “Fig. 5”. As can be seen, the most effective geometrical parameter on the excitability is the ratio of  $L_1/L$ . Therefore, this parameter is an important geometric parameter in designing piezoelectric MCs and optimizing its properties. In addition to the length of piezoelectric layer, the thickness of the piezoelectric is an effective geometric property, which has to be considered in designing optimum MC.

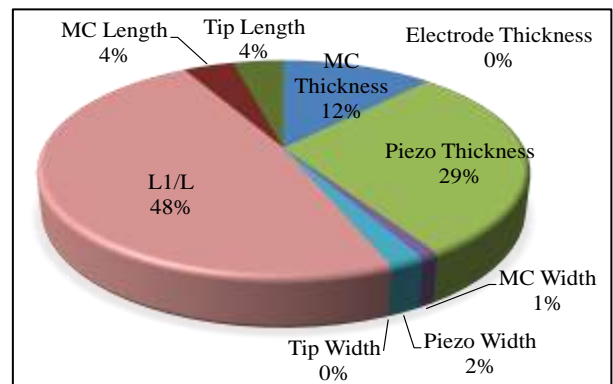


Fig. 5 Sensitive percentage of excitability to geometric dimensions of MC.

4 CONCLUSIONS

Vibrating behavior of MC as nano-resonator was modeled and investigated. In order to model the vibrating motion of MC, Hamilton principle and Euler-Bernoulli theory were applied. Since, in this type of MCs, the tip has smaller width to enhance the sensitivity, piezoelectric layer doesn't cover the MC. Therefore, MC has a geometric discontinuity that must be considered in dynamic modeling. Accordingly, the differential Equation of motion was solved considering geometrical discontinuities of MC with Galerkin approximation and with respect to continuity conditions. In order to study the effects of geometry on the excitability of MC, statistical eFAST sensitivity analysis method was conducted. Sensitivity analysis results show that  $L_1/L$  and thickness of piezoelectric layer are the most influential geometrical parameters on the excitability of

MCs. These parameters have to be taken into account in the design and selection of MCs. The width of MC and the tip are the least influential parameters, therefore they can be given lower priority in design and selection of MCs. According to the results of the sensitivity analysis, when the length of MC is equal to 490 micrometers, and  $L_1/L=0.74$ , the excitability of MC is maximized. To enhance the excitability, it is recommended to select a narrow and long tip for MC. According to the results, the increase in the thickness of MC increases its excitability.

5 APPENDIXES

Description of characteristic matrix:

$$\text{Jacob} = \begin{bmatrix}
 0 & 0 & 0 & 0 & 0 & 0 & 0 \\
 0 & 0 & 0 & 0 & 0 & 0 & 0 \\
 0 & 0 & 0 & 0 & 0 & \text{Sin}\alpha_2 L_2 \Omega & \text{Cos}\alpha_2 L_2 \Omega \\
 0 & 0 & 0 & 0 & 0 & \gamma_2 \text{Cos}\alpha_2 L_2 \Omega & -\gamma_2 \text{Sin}\alpha_2 L_2 \Omega \\
 0 & 0 & 0 & 0 & 0 & -\gamma_2^2 \text{Sin}\alpha_2 L_2 \Omega & -\gamma_2^2 \text{Cos}\alpha_2 L_2 \Omega \\
 0 & 0 & 0 & 0 & 0 & \gamma_2^3 \text{Cos}\alpha_2 L_2 \Omega & \gamma_2^3 \text{Sin}\alpha_2 L_2 \Omega \\
 \text{Sin}\alpha_1 L_1 \Omega & \text{Cos}\alpha_1 L_1 \Omega & \text{Sin}\alpha_1 L_1 \Omega & \text{Cosh}\alpha_1 L_1 \Omega & -\text{Sin}\alpha_2 L_1 \Omega & -\text{Cos}\alpha_2 L_1 \Omega \\
 \gamma_1 \text{Cos}\alpha_1 L_1 \Omega & -\gamma_1 \text{Sin}\alpha_1 L_1 \Omega & \gamma_1 \text{Coh}\alpha_1 L_1 \Omega & \gamma_1 \text{Sin}\alpha_1 L_1 \Omega & -\text{Cos}\alpha_2 L_1 \Omega & \text{Sin}\alpha_2 L_1 \Omega \\
 -\gamma_1^2 \text{Sin}\alpha_1 L_1 \Omega & -\gamma_1^2 \text{Cos}\alpha_1 L_1 \Omega & \gamma_1^2 \text{Sin}\alpha_1 L_1 \Omega & \gamma_1^2 \text{Cosh}\alpha_1 L_1 \Omega & \text{Sin}\alpha_2 L_1 \Omega & \text{Cos}\alpha_2 L_1 \Omega \\
 \gamma_1^3 \text{Cos}\alpha_1 L_1 \Omega & \gamma_1^3 \text{Sin}\alpha_1 L_1 \Omega & \gamma_1^3 \text{Coh}\alpha_1 L_1 \Omega & \gamma_1^3 \text{Sin}\alpha_1 L_1 \Omega & \text{Cos}\alpha_2 L_1 \Omega & -\text{Sin}\alpha_2 L_1 \Omega \\
 0 & 1 & 0 & 1 & 0 & -1 \\
 1 & 0 & 1 & 0 & 1 & 0 \\
 0 & 0 & -\text{Cos}\alpha_3 L \Omega & \text{Sin}\alpha_3 L \Omega & \text{Cosh}\alpha_3 L \Omega & \text{Sin}\alpha_3 L \Omega \\
 0 & 0 & -\text{Sin}\alpha_3 L \Omega & -\text{Cos}\alpha_3 L \Omega & \text{Sin}\alpha_3 L \Omega & \text{Cosh}\alpha_3 L \Omega \\
 \text{Sin}\alpha_2 L_2 \Omega & \text{Cosh}\alpha_2 L_2 \Omega & -\text{Sin}\alpha_3 L_2 \Omega & -\text{Cos}\alpha_3 L_2 \Omega & -\text{Sin}\alpha_3 L_2 \Omega & -\text{Cosh}\alpha_3 L_2 \Omega \\
 \gamma_2 \text{Cos}\alpha_2 L_2 \Omega & \gamma_2 \text{Sin}\alpha_2 L_2 \Omega & -\text{Cos}\alpha_3 L_2 \Omega & \text{Sin}\alpha_3 L_2 \Omega & -\text{Cosh}\alpha_3 L_2 \Omega & -\text{Sin}\alpha_3 L_2 \Omega \\
 \gamma_2^2 \text{Sin}\alpha_2 L_2 \Omega & \gamma_2^2 \text{Cos}\alpha_2 L_2 \Omega & \text{Sin}\alpha_3 L_2 \Omega & \text{Cos}\alpha_3 L_2 \Omega & -\text{Sin}\alpha_3 L_2 \Omega & -\text{Cosh}\alpha_3 L_2 \Omega \\
 \gamma_2^3 \text{Cosh}\alpha_2 L_2 \Omega & \gamma_2^3 \text{Sin}\alpha_2 L_2 \Omega & \text{Cos}\alpha_3 L_2 \Omega & -\text{Sin}\alpha_3 L_2 \Omega & -\text{Cosh}\alpha_3 L_2 \Omega & -\text{Sin}\alpha_3 L_2 \Omega \\
 -\text{Sin}\alpha_2 L_1 \Omega & -\text{Cosh}\alpha_2 L_1 \Omega & 0 & 0 & 0 & 0 \\
 -\text{Cosh}\alpha_2 L_1 \Omega & -\text{Sin}\alpha_2 L_1 \Omega & 0 & 0 & 0 & 0 \\
 -\text{Sin}\alpha_2 L_1 \Omega & -\text{Cosh}\alpha_2 L_1 \Omega & 0 & 0 & 0 & 0 \\
 -\text{Cosh}\alpha_2 L_1 \Omega & -\text{Sin}\alpha_2 L_1 \Omega & 0 & 0 & 0 & 0 \\
 0 & -1 & 0 & 0 & 0 & 0 \\
 -1 & 0 & 0 & 0 & 0 & 0
 \end{bmatrix} \tag{A.1}$$

Where:

$$\alpha_i = \sqrt[4]{\frac{m_i}{(EI)_i}} / L; \quad \gamma_i^n = \frac{(EI)_i}{(EI)_{i+1}} \left( \frac{\alpha_i}{\alpha_{i+1}} \right)^{n-1}; \tag{A.2}$$

$$\Omega = \omega_n^{1/2}$$

## REFERENCES

- [1] Yilmaz, C., Sahin, R., and Topal, E. S., Exploring the Static Acoustic Force Sensitivity Using Afm Micro-Cantilever Under Single-And Bimodal-Frequency Excitation, *Measurement Science and Technology*, Vol. 32, No. 11, 2021, pp. 115001.
- [2] Alibakhshi, A., et al., Nonlinear Free and Forced Vibrations of a Dielectric Elastomer-Based Microcantilever for Atomic Force Microscopy, *Continuum Mechanics and Thermodynamics*, 2022, pp. 1-18.
- [3] Ghaderi, R., Dehkordi, B. M., and Fard, A. R., Vibration and Sensitivity Analysis of Double-Layered Non-Uniform Piezoelectric Microcantilever as a Self-Sensing Mass Sensor, *Physica Scripta*, Vol. 96, No. 11, 2021, pp. 115205.
- [4] Mistry, K., et al., Highly Sensitive Self-Actuated Zinc Oxide Resonant Microcantilever Humidity Sensor. *Nano letters*, Vol. 22, No. 8, 2022, pp. 3196-3203.
- [5] Jia, H., Xu, P., and Li, X., Integrated Resonant Micro/Nano Gravimetric Sensors for Bio/Chemical Detection in Air and Liquid. *Micromachines*, Vol. 12, No. 6, 2021, pp. 645.
- [6] Moshirpanahi, A., Haghghi, S. E., and Imam, A., Dynamic Modeling of a Cylindrical Nanoparticle Manipulation by AFM, *Engineering Science and Technology, an International Journal*, Vol. 24, No. 3, 2021, pp. 611-619.
- [7] Mohammadi, S. Z., Moghadam, M., and Pishkenari, H. N., Dynamical Modeling of Manipulation Process in Trolling-Mode AFM, *Ultramicroscopy*, Vol. 197, 2019, pp. 83-94.
- [8] Rotake, D., Darji, A., and Kale, N., Fabrication, Calibration, and Preliminary Testing of Microcantilever-Based Piezoresistive Sensor for BioMEMS Applications, *IET Nanobiotechnology*, Vol. 14, No. 5, 2020, pp. 357-368.
- [9] Kasambe, P., Bhole, K., and Bhoir, D., Analytical Modelling, Design Optimisation and Numerical Simulation of a Variable Width Cantilever Beam MEMS Switch, *Advances in Materials and Processing Technologies*, 2021, pp. 1-21.
- [10] Angira, M., et al., A Novel Capacitive Rf-Mems Switch for Multi-Frequency Operation, *Superlattices and Microstructures*, Vo. 133, 2019, pp. 106204.
- [11] Caruntu, D. I., et al., Frequency–Amplitude Response of Superharmonic Resonance of Second Order of Electrostatically Actuated MEMS Cantilever Resonators, *International Journal of Non-Linear Mechanics*, Vol. 133, 2021, pp. 103719.
- [12] Park, C., et al., Highly Sensitive and Selective Detection of Single-Nucleotide Polymorphisms Using Gold Nanoparticle MutS Enzymes and a Micro Cantilever Resonator, *Talanta*, Vol. 205, 2019, pp. 120154.
- [13] Mahmoodi Nasrabadi, H., et al., High Resolution Atomic Force Microscopy with an Active Piezoelectric Microcantilever, *Review of Scientific Instruments*, Vol. 93, No. 7, 2022, pp. 073706.
- [14] Niranjana, A., Gupta, P., and Rajoriya, M., Piezoelectric MEMS Micro-Cantilever Biosensor for Detection of SARS–CoV2. in *2021 International Conference on Communication, Control and Information Sciences (ICCISc)*, IEEE, 2021.
- [15] Katta, M., Sandanalakshmi, R., Simultaneous Tropical Disease Identification with PZT-5H Piezoelectric Material Including Molecular Mass Biosensor Microcantilever Collection, *Sensing and Bio-Sensing Research*, Vol. 32, 2021, pp. 100413.
- [16] Manalis, S., Minne, S., and Quate, C., Atomic Force Microscopy for High Speed Imaging Using Cantilevers with an Integrated Actuator and Sensor, *Applied Physics Letters*, Vol. 68, No. 6, 1996, pp. 871-873.
- [17] Rogers, B., et al., Improving Tapping Mode Atomic Force Microscopy with Piezoelectric Cantilevers, *Ultramicroscopy*, Vol. 100, No. 3-4, 2004, pp. 267-276.
- [18] Wolf, K., Gottlieb, O., Nonlinear Dynamics of a Noncontacting Atomic Force Microscope Cantilever Actuated by a Piezoelectric Layer, *Journal of Applied Physics*, Vol. 91, No. 7, 2002, pp. 4701-4709.
- [19] Fung, R. F., Huang, S. C., Dynamic Modeling and Vibration Analysis of The Atomic Force Microscope, *J. Vib. Acoust.*, Vol. 123, No. 4, 2001, pp. 502-509.
- [20] Mahmoodi, S. N., Afshari, M., and Jalili, N., Nonlinear Vibrations of Piezoelectric Microcantilevers for Biologically-Induced Surface Stress Sensing, *Communications in Nonlinear Science and Numerical Simulation*, Vol. 13, No. 9, 2008, pp. 1964-1977.
- [21] Mahmoodi, S. N., Jalili, N., Piezoelectrically Actuated Microcantilevers: an Experimental Nonlinear Vibration Analysis, *Sensors and Actuators A: Physical*, Vol. 150, No. 1, 2009, pp. 131-136.
- [22] Mahmoodi, S. N., Jalili, N., and Ahmadian, M., Subharmonics Analysis of Nonlinear Flexural Vibrations of Piezoelectrically Actuated Microcantilevers, *Nonlinear Dynamics*, Vol. 59, No. 3, 2010, pp. 397-409.
- [23] Salehi-Khojin, A., Bashash, S., and Jalili, N., Modeling and Experimental Vibration Analysis of Nanomechanical Cantilever Active Probes, *Journal of Micromechanics and Microengineering*, Vol. 18, No. 8, 2008, pp. 085008.